Sakarya Üniversitesi Fen Bilimleri Dergisi
Sakarya University Journal of Science

e-ISSN : 2147-835X
Publisher : Sakarya University

Vol. 29, No. 5, 550-561, 2025
DOI: https://doi.org/10.16984/saufenbilder.1738801

Research Article

Investigation of Hydrogen Adsorption Mechanism on Activated Carbon Surface Using Isotherm and Kinetic Models

Zeynep Bicil

Balıkesir University, Faculty of Science and Literature, Department of Chemistry, Balıkesir, Türkiye, zeynepbicil@balikesir.edu.tr, ror.org/02tv7db43
*Corresponding Author

ARTICLE INFO

Keywords:
Tangerine peel
Horse chestnut shell
Activated carbon
Hydrogen storage
Kinetic

Article History:
Received: 09.07.2025
Revised: 08.09.2025
Accepted: 16.09.2025
Online Available: 21.10.2025

ABSTRACT

In this study, the hydrogen storage capacities and adsorption behaviors of activated carbons obtained from agricultural wastes such as tangerine peel and horse chestnut were investigated in detail. The carbons were synthesized by chemical activation using $ZnCl_2$ and characterized by BET surface area and pore analysis. The hydrogen storage capacities of activated carbons produced by chemical activation and carbonization processes were measured as a function of pressure at 77 K up to 80 bar. Horse chestnut-based activated carbon showed higher performance with a maximum hydrogen adsorption capacity of 4.47% at 80 bar, whereas tangerine peel-based activated carbon reached only 1.87% at 26 bar. Adsorption data were analyzed with Langmuir, Freundlich and Temkin isotherm models; the Langmuir model provided the highest fit ($R^2 > 0.99$) for both samples. In kinetic analyses, high correlation was obtained with pseudo-second-order and Weber–Morris models. The findings reveal the effectiveness of biomass-based activated carbons in the storage of hydrogen by physical adsorption and contribute to both theoretical and applied aspects of adsorption processes. In this respect, the study provides a scientific basis for the development of environmentally friendly and low-cost adsorbents that can be used in sustainable energy technologies.

1. Introduction

Energy is the driving force of industrialization as one of the fundamental dynamics of economic development and social welfare today. With population growth, industrialization and technological developments, energy demand is increasing rapidly; this situation necessitates a shift towards sustainable, environmentally friendly and economical energy sources [1]. Energy sources are generally divided into two main categories: renewable and non-renewable. The limited reserves of fossil fuels, environmental damage and market instabilities increase the interest in alternative solutions [2]. In this context, renewable energy sources such as solar, wind, geothermal, biomass and hydrogen are considered as strategic options in terms of environmental sustainability and energy security [3, 4].

The use of renewable resources plays an active role in combating climate change by reducing greenhouse gas emissions. In addition, it is important for the continuity of energy supply that resources such as solar and wind are not limited to direct electricity production but also used in the production of storable energy carriers [5]. In this context, hydrogen is a prominent energy carrier thanks to its high energy density of 120 MJ/kg, its clean combustion product that produces only water vapor, and its diverse production methods [6, 7].

However, making hydrogen usable in practice requires the development of efficient and safe storage technologies. Current hydrogen storage methods are divided into three main groups: compression under high pressure in the gas phase, condensation at low temperatures in the

Cite as: Z. Bicil, "Investigation of hydrogen adsorption mechanism on activated carbon surface using isotherm and kinetic models," Sakarya University Journal of Science, vol. 29, no. 5, pp. 550-561, 2025. https://doi.org/10.16984/saufenbilder.1738801

liquid phase, and chemical or physical adsorption in the solid phase [8]. Each of these methods has its own advantages and limitations. For example, high-pressure gas storage systems require complex engineering infrastructure, while liquefied hydrogen systems have high energy costs due to the extremely low temperature requirement of -253 °C. Although chemical storage methods (e.g. metal hydrides) can reach high capacities, they are limited in terms of reversibility and reaction kinetics. Therefore, solid-phase physical adsorption has been considered as an alternative that has attracted great interest in recent years due to its low energy requirement, rapid recovery, safe transportation and environmentally friendly nature [9].

The main adsorbent materials in physical adsorption-based hydrogen storage systems are metal-organic frameworks (MOF), zeolites, boron hydrides, carbides and carbon derivatives [7, 10-14]. Among these groups, carbon-based adsorbents are prominent candidates with their high surface area, low cost, chemical stability and structureable pore properties [1, 15-16]. In addition, activated carbons obtained by carbonizing agricultural wastes offer additional advantages in terms of environmental sustainability and circular economy principles [17, 18].

In recent years, the hydrogen adsorption properties of activated carbons produced from biomass sources such as tangerine peel [16], olive leaf [7], coconut shell [19], almond shell [1] and horse chestnut shell [18] have been investigated. However, in these studies, only the storage capacity is usually reported, and adsorption isotherms and kinetic behaviors are not analyzed. Nevertheless, these parameters play a critical role in understanding the interaction of hydrogen with the surface and the adsorptive efficiency of the system [20]. Thus, the aim of this study is to fill this literature gap and to investigate in detail the hydrogen storage behaviors of activated carbons obtained from tangerine peel and horse chestnut in terms of both capacity and adsorption kinetics.

Adsorption processes were analyzed using Langmuir, Freundlich and Temkin isotherm models and several kinetic models (pseudo-first-order, pseudo-second-order, Boyd, Avrami and Weber–Morris). The results showed that horse chestnut–based activated carbon exhibited a higher hydrogen storage capacity (4.47 wt. % at 80 bar) compared to tangerine peel–based carbon, and the Langmuir and pseudo-second-order models best explained the adsorption behavior. These findings highlight that biomass-derived carbons can be effective and sustainable candidates for hydrogen storage applications.

2. General Methods

In this study, two different biomass sources, horse chestnut and tangerine peel, were used to produce activated carbon. Zinc chloride ($ZnCl_2$) used as the activation agent was supplied by Sigma-Aldrich.

2.1. Synthesis of activated carbons

Horse chestnut and tangerine peels were first washed with plenty of water to remove impurities and then dried at 110 ° C. Dried biomasses were ground in a Retsch PM100 brand ball mill and sieved in a Retsch AS200 device to a particle size range of 100–500 μm.

Horse chestnut shell was impregnated with $ZnCl_2$ at a ratio of 1:4 (1 g biomass with 4 g $ZnCl_2$ dissolved in 40 mL distilled water) by chemical activation method, then subjected to preheating at 220°C, then kept at room temperature for 24 hours to break down the lignocellulosic structure. After pretreatment, the sample was pyrolyzed at 600°C under nitrogen atmosphere for 2 hours. The activated carbon obtained after pyrolysis was washed with pure water until pH 7 was reached in order to remove excess $ZnCl_2$ and dried at 110°C [18].

The tangerine peel (25 g) was kept at room temperature for 24 hours with 5 M $ZnCl_2$ solution (50 ml) and then dried at 110°C. The dried sample was pyrolyzed at 700°C in an inert nitrogen atmosphere for 2 hours. The active carbon obtained after pyrolysis was washed with pure water and dried at 110°C [16]. The chemical activation method was preferred because it enables better pore development and higher surface area at lower activation temperatures compared to physical activation, making it more

suitable for hydrogen adsorption applications. $ZnCl_2$ was chosen as the activating agent since it decomposes cellulose and facilitates the formation of micropores, leading to higher surface area in the activated carbons [1].

2.2. Characterization

BET surface area measurements and pore size analyses of activated carbons were obtained using a Quantachrome Nova brand 2200e series device. Measurements of activated carbons, which were degassed at 105°C for 24 hours before analysis, were carried out using nitrogen gas at 77 K.

2.3. Hydrogen storage analysis

Hydrogen adsorption measurements of activated carbons were carried out in a Hiden IMI PSI brand hydrogen storage device at 77 K. Before analysis, the materials were degassed at 105°C for 4 hours.

3. Results and Discussion

3.1.Hydrogen storage

Table 1 shows the hydrogen storage capacities of activated carbons produced from horse chestnut and tangerine peel at cryogenic temperature. Hydrogen storage analyses of activated carbons were carried out at pressures between 0 and 80 bar and remarkable results were obtained in terms of storage capacity. Activated carbon produced from horse chestnut shells exhibited a very high storage capacity with a hydrogen storage capacity of 1.90% by weight at 1 bar, 4.24% at 20 bar and a maximum of 4.47% at 80 bar. Tangerine peel-based activated carbon, on the other hand, exhibited a lower performance with a capacity of 0.89% by weight at 1 bar, 1.84% at 20 bar and a maximum of 1.87% at 26 bar. The basis of these differences lies in the surface properties of the materials and the separation in their pore structures. The N_2 adsorption-desorption isotherms presented in Figure 1 and the characterization data given in Table 1 provide information about the surface area and pore volumes of the mentioned activated carbons. The BET surface area of the horse chestnut-based activated carbon was determined as 2128 m^2/g, while this value was at the level of 1230 m^2/g for the tangerine peel-based activated carbon. This difference in surface area is due to the structural properties that develop depending on the pretreatment steps, activation parameters and biomass type.

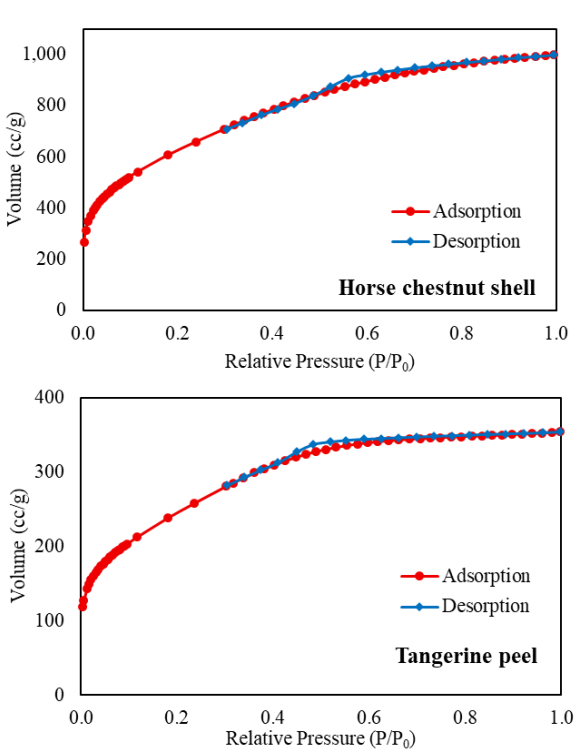

Figure 1. N_2 adsorption-desorption isotherms of activated carbons

Table 1. BET surface areas of activated carbons and hydrogen storage capacities at different pressures

Sample name	S_{BET} (m^2/g)	V_t (cc/g)	V_{micro} (cc/g)	V_{DFT} (cc/g)	V_{meso} (cc/g)	H_2 % (w/w) (1 bar)	H_2 % (w/w) (20 bar)	**Maximum value** H_2 % (w/w)	Pressure (bar)
Horse chestnut shell	2128	1.55	0.88	1.42	0.54	1.90	4.24	4.47	80
Tangerine peel	1230	0.55	0.36	0.49	0.13	0.89	1.84	1.87	26

Detailed information about the pore structure is supported by the cumulative pore volume-pore diameter distribution graph obtained using the Density Functional Theory (DFT) method, as presented in Figure 2. The micropore volume of the horse chestnut-based activated carbon was calculated as 0.88 cm^3/g and the mesopore volume as 0.54 cm^3/g. The activated carbon

produced from tangerine peel has a micropore volume of 0.36 cm³/g and a mesopore volume of 0.13 cm³/g. These data show that the horse chestnut-based sample has not only a larger surface area but also a more developed pore volume and a more balanced micro/mesopore distribution. In particular, the ability of micropores to effectively adsorb hydrogen molecules ensures that high adsorption capacity is achieved in such structures.

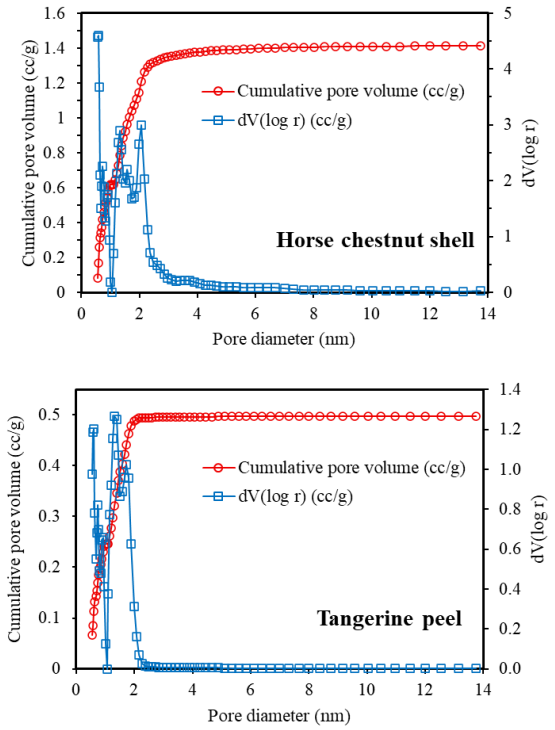

Figure 2. DFT pore size distribution graphs of activated carbons

Figure 3 shows the hydrogen adsorption isotherms of activated carbons at 77 K. When the figure is examined, it is observed that hydrogen adsorption increases with pressure for both activated carbons, but the rate of increase decreases after a certain point. This can be associated with the saturation of active points at high pressures. Activated carbon from horse chestnut was able to perform effective adsorption even at low pressures due to its high surface area and porosity. In addition, the material's micro and mesopore balance allowed the adsorption of hydrogen both on the surface and in the pores. On the other hand, activated carbon from tangerine peel reached a more limited hydrogen storage capacity due to its low surface area and low porosity. This clearly shows that the type of biomass and the applied activation methods are the determining factors in adsorption performance. While the rapid adsorption observed in horse chestnut activated carbon indicates the high affinity and accessibility of the surface, the tangerine peel-based activated carbon sample reaches surface saturation early.

These results show that waste biomass can be converted into high-performance hydrogen storage materials with appropriate activation methods. In addition, such materials offer low-cost and environmentally friendly alternatives in energy storage systems. In the hydrogen storage processes that occur on the surfaces and pores of activated carbon at cryogenic temperatures, physical adsorption (physisorption) interactions mainly occur between the hydrogen molecules and the activated carbon surface [16]. These interactions are based on weak and reversible forces such as van der Waals forces. Low temperature reduces the kinetic energy of hydrogen molecules, allowing them to adhere more easily to the carbon surface and increasing the adsorption capacity [1]. Microporous structures in particular offer local areas with high surface energy to effectively adsorb hydrogen molecules. Therefore, activated carbons with high surface area and well-optimized pore size distribution can adsorb more hydrogen at cryogenic temperatures. However, since there is no chemical bonding in this process, adsorption and desorption processes are fast and easy.

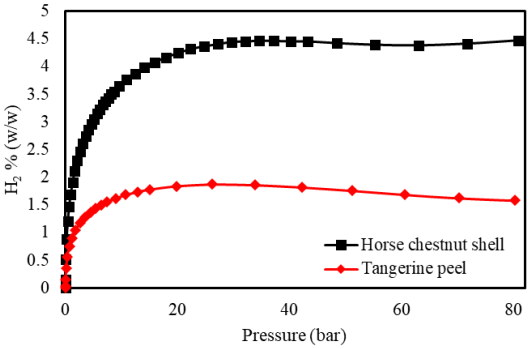

Figure 3. Hydrogen adsorption isotherms of activated carbons

The hydrogen adsorption data obtained in this study were also evaluated by comparing with various biomass-based carbon materials previously reported in the literature (Table 2). The hydrogen storage capacity of the samples in the table varies significantly depending on the

structural properties of the adsorbent such as surface area, pore size distribution, surface chemistry and activation method. According to the data in the table, pinecone has the highest hydrogen storage capacity with 5.25% (w/w), and this value was obtained as a result of experiments carried out under high pressure [21]. In this study, the activated carbon sample produced from horse chestnut shell has a storage capacity of 4.47% by weight, which is lower than pine cone-based activated carbon but higher than many samples such as coffee bean waste (4.00%) [22], almond shell (2.53%) [1] and olive pulp (2.59%) [23]. This result reveals that the surface properties and pore structure of horse chestnut activated carbon are extremely suitable for hydrogen adsorption.

Table 2. Hydrogen storage capacities of some biomass-based activated carbons at 77 K

Materials	**Max. value**		Ref
	H_2 % wt.	P (bar)	
Almond shell	2.53	27	[1]
Pine cone	5.25	80	[21]
Coffee bean waste	4.00	40	[22]
Olive bagasse	2.59	25	[23]
Fruit bunch	2.14	20	[24]
Mandarin fruit	1.90	25	[25]
Horse chestnut shell	4.47	80	In this study
Tangerine peel	1.87	26	In this study

Examples with medium hydrogen storage capacity include fruit bunch (2.14%) [24] and tangerine fruit (1.90%) [25]. Although the tangerine peel-based activated carbon evaluated in this study was tested under low pressure conditions with a capacity of 1.87%, it gave similar results with some samples. Although they offer low capacity, these types of agricultural wastes are among the alternative raw materials that can be evaluated in sustainable energy applications due to their low cost and bioavailability. The differences observed between materials in terms of hydrogen storage capacity are related not only to the chemical structure but also to the effects of the applied carbonization and activation processes. The high capacity of pine cone and horse chestnut shell samples tested at high pressure confirms that adsorption pressure is a determining parameter. Under high pressure, effective filling of micropores in carbon structures is ensured and hydrogen storage efficiency increases. As a result, activated carbon produced from horse chestnut shell within the scope of this study has only lower capacity than pine cone in terms of hydrogen storage capacity and higher storage capacity than all other samples in the table. In this context, horse chestnut shell can be considered as a sustainable, environmentally friendly and economical hydrogen storage material. On the other hand, materials with relatively low capacity such as tangerine peel can be made more efficient by surface modifications and porosity-enhancing processes.

3.2. Isotherm analysis

Understanding the adsorption behavior of hydrogen on solid surfaces is of great importance to evaluate the potential of these materials in energy storage applications. Hydrogen adsorption isotherms are used to explain the interaction of the amount of hydrogen held at different pressures at a certain temperature with the surface. With these isotherm models, quantitative assessments can be made about the adsorption capacity and the type and intensity of surface-adsorbate interaction. In addition, by comparing the agreement of different models with experimental data, inferences can be obtained about the mechanism of the adsorption process [26].

The Langmuir isotherm is a model based on the assumption of a monolayer and homogeneous surface developed to explain gas adsorption on solid surfaces. In this model, it is assumed that all active sites on the adsorption surface have equal energy and that each site can be occupied by only one molecule [27]. This model, which is developed assuming that there is no interaction between molecules, gives good results especially at low pressure conditions. The linearized mathematical expression of the isotherm is given below:

$$\frac{P}{n} = \frac{1}{n_m B} + \frac{P}{n_m} \quad (1)$$

In the equation, P represents the partial equilibrium pressure, n_m represents the monolayer adsorption capacity, n represents the amount of adsorbate adsorbed by the unit mass of the layer, and B represents the Langmuir constant.

The Freundlich isotherm model is an empirical model that assumes that adsorption occurs in multiple layers on heterogeneous solid surfaces. According to this model, adsorption first occurs on regions with high binding energy; as adsorption increases, the binding strength of the active sites on the surface decreases. This model, which is generally valid in low and medium pressure ranges, is especially useful in systems with inhomogeneous surfaces [28]. The linearized Freundlich isotherm equation is given below:

$$\ln(n) = \ln(K_F) + \frac{1}{n_F}\ln(P) \quad (2)$$

In the relevant equation, K_F is the Freundlich constant and n is the amount of adsorbate adsorbed. Temkin isotherm model takes into account the interactions between adsorbent and adsorbate during adsorption. The model assumes that the heat of adsorption does not remain constant as surface coverage increases but decreases linearly. In this respect, it differs from the Langmuir model and is particularly suitable for use at moderate surface saturations. Temkin constants can be calculated from graphs where the amount of adsorption is plotted logarithmically against pressure [28]. The isotherm equation is given below.

$$n = B\ lnA_T + B\ln P \quad (3)$$

In this equation, Temkin isotherm equilibrium binding constant is symbolized by A_T and the constant related to the heat of adsorption is symbolized by B.

The regression coefficients and isotherm parameters obtained by applying the experimental data to the Langmuir, Freundlich and Temkin isotherms are given in Table 3.
In addition, the linearized Langmuir isotherm plots for both activated carbons are presented in Figure 4. The Langmuir isotherm model was the model that best explained the hydrogen adsorption data by showing high regression coefficients for both biomass-based activated carbons (R^2 = 0.9920 and 0.9955). The Freundlich isotherm showed a lower level of fit (R^2 = 0.9626 and 0.8991), while the correlation coefficients of the Temkin model (R^2 = 0.9206 and 0.9662) showed a moderate fit. The Langmuir model is a model that assumes that adsorption occurs on single-layered surfaces with homogeneous energy and that there is no interaction between the adsorbed molecules [29]. These high correlation coefficients indicate that the surfaces establish regular and reversible interactions with hydrogen. When the model parameters are evaluated, the maximum adsorption capacity (n_m) of the horse chestnut shell-based activated carbon is calculated as 4.53 (%wt.).

This value is approximately 2.4 times higher than the capacity of 1.90 of the activated carbon produced from tangerine peel. This shows that the horse chestnut adsorbent has a larger surface area and a suitable pore structure. The Langmuir constant (B) is related to the surface-adsorbate interaction energy; this constant was higher in tangerine peel (0.79), which may indicate stronger local interactions. However, the low total surface area and capacity suggest that this advantage has limited contribution to storage performance. Such results have also been observed in previous studies on activated carbon and carbon-derived materials [30]. As a result, the Langmuir model is the model that best explains the regular and monolayer binding of hydrogen to both biomass-based adsorbents. Especially horse chestnut shell-based activated carbon stands out as a more suitable candidate for hydrogen storage applications with both its high adsorption capacity and high compliance with the Langmuir isotherm.

Table 3. Hydrogen adsorption isotherm data of activated carbons

Sample name	Langmuir			Freundlich			Temkin		
	n_m (%wt.)	B	R^2	n_F	K_F	R^2	A_T	B	R^2
Horse chestnut shell	4.53	0.53	0.9920	2.27	1.37	0.9626	0.57	2.18	0.9206
Tangerine peel	1.90	0.79	0.9955	2.27	0.64	0.8991	0.25	0.99	0.9662

This result is consistent with the findings in the literature that microporous carbon materials have a high hydrogen storage potential under low temperature and medium pressure conditions [1]. Thus, it has been confirmed once again that biomass-based carbon materials offer strong alternatives in terms of sustainable and environmentally friendly hydrogen storage solutions.

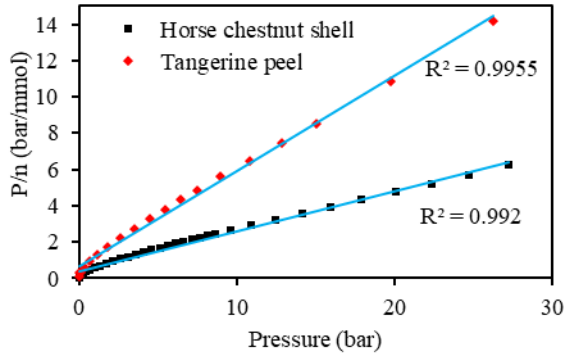

Figure 4. Langmuir isotherm plots for hydrogen adsorption on activated carbons

3.3.Adsorption kinetic

In gas phase adsorption processes, molecular interactions occurring during the contact period are the basic elements affecting the adsorption rate. Figure 5 shows the change in hydrogen adsorption capacities of horse chestnut and tangerine peel based activated carbon samples under different pressures. For both adsorbents, the adsorption process shows a rapid increase at the beginning of the contact period. At this stage, gas molecules are easily adsorbed to the active points on the surface and the adsorption amount increases over time. This rapid increase at the beginning is related to the surface being largely empty and accessible. As time progresses, the possibility of molecules reaching the surface decreases as the suitable areas on the surface decrease. This causes the adsorption rate to slow down. After a certain period of time, the system reaches equilibrium and no significant change is observed in the adsorption amount over time. At this stage, equilibrium is established between the adsorption and desorption processes.

Kinetic models are widely used to understand adsorption processes. In this study, the adsorption behavior of hydrogen gas onto activated carbon samples was analyzed by pseudo-first-order and pseudo-second-order kinetic models. Both models were derived from chemical reaction kinetics and applied to time-varying adsorption data, and the results are presented in Table 4. The pseudo-first-order kinetic model assumes that the adsorption rate is proportional to the difference between the adsorbed amount (q_e) at equilibrium and the adsorbed amount (q_t) at any instant. The linear form of the model is:

$$\ln(q_e - q_t) = \ln q_e - k_1 t \quad (4)$$

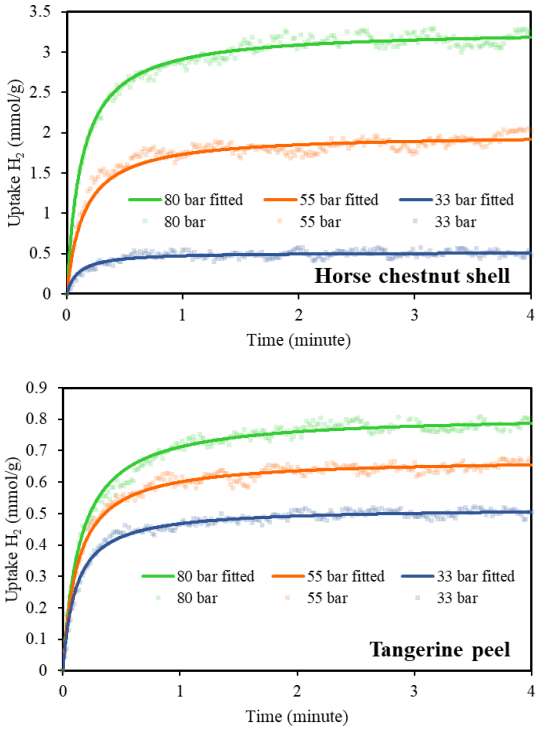

Figure 5. Change in hydrogen adsorption amounts of activated carbons with time at different pressures

In this equation, q_t is the amount adsorbed at time t (mmol/g); q_e is the amount adsorbed at equilibrium (mmol/g); k_1 is the pseudo-first-order rate constant (minute^{-1}), and t is the time (minute). This model generally gives more appropriate results when the amount of adsorbed substance is low compared to the adsorbent capacity. The correlation coefficients (R^2) obtained as a result of the application showed moderate agreement in some examples but generally remained at low values (Table 4).

The pseudo-second-order kinetic model assumes that the adsorption rate is proportional to the square of the amount of adsorbed material and is

generally suitable for systems with high surface capacity. The linear form of the equation is:

$$\frac{t}{q_t} = \frac{1}{k_2 q_e^2} + \frac{t}{q_e} \quad (5)$$

In the relevant equation, k_2 is the pseudo-second order rate constant (g mmol^{-1} min^{-1}). According to the equation, the plot of t/q_t against t should give a straight line with a slope of $1/q_e$ and an extrapolation of $1/(k_2 q_e^2)$. Figure 6 shows the plots of t/q_t against t for horse chestnut and tangerine peel based activated carbons using the pseudo-second order kinetic model. In both graphs, the experimental data obtained for hydrogen adsorption under different pressure conditions show a linear distribution. The high correlation coefficients of the obtained linear graphs ($R^2 = 0.9769–0.9982$) and the closeness of the curves to the experimental points show that the pseudo-second order kinetic model successfully represents the systems.

Which step in the adsorption process is the rate-determining step is of critical importance both for understanding the mechanism and for industrial applications. Especially in gas phase applications, how quickly and by what mechanism the adsorbed substance is transported to the surface directly affects the design, storage and recovery processes. In this study, Boyd, Avrami and Weber–Morris models were used to evaluate the adsorption mechanism.

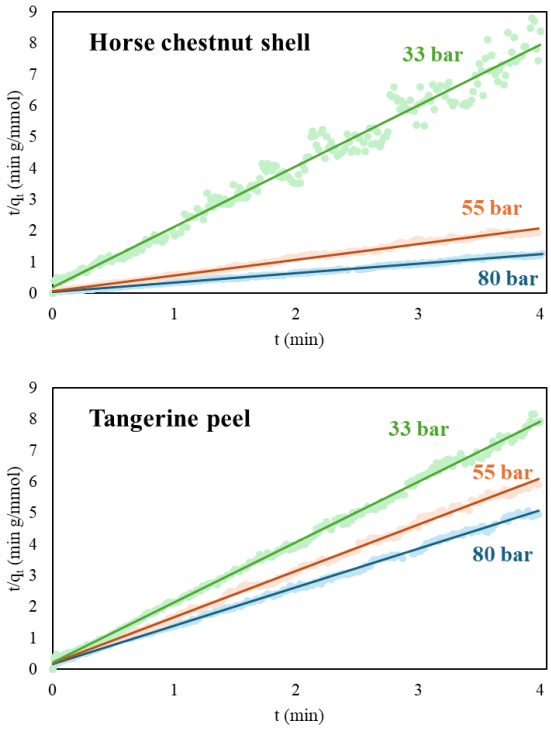

Figure 6. t/q_t–t curves plotted according to the pseudo-second-order kinetic model for activated carbons at different pressures

Table 4. Kinetic parameters for the adsorption of hydrogen on the surface of activated carbons

Sample name	Pressure (bar)	Pseudo-first order			Pseudo-second order			
		R^2	$q_{e(cal)}$ (mmol/g)	k_1	R^2	$q_{e(exp)}$ (mmol/g)	$q_{e(cal)}$ (mmol/g)	k_2
Horse chestnut shell	80	0.6451	4.083	1.13	0.9974	3.336	3.283	2.40
	55	0.6533	1.176	1.44	0.9932	2.081	1.984	3.43
	33	0.2652	0.356	1.12	0.9769	0.602	0.516	20.03
Tangerine peel	80	0.7120	0.082	1.17	0.9982	0.822	0.815	8.45
	55	0.7249	0.027	1.24	0.9981	0.683	0.675	11.91
	33	0.6500	0.019	1.18	0.9979	0.528	0.518	17.58

Boyd model is an approach to distinguish whether adsorption occurs on the outer surface (film diffusion) or in the inner regions (intrapore diffusion). The logarithmic form of the model is given below:

$$\ln\left(1 - \frac{q_t}{q_e}\right) = -Rt + A \quad (6)$$

Here R represents the rate constant and A represents the Boyd constant. According to the equation, if the plot of $\ln(1-q_t/q_e)$ versus t is linear, film diffusion is considered to be the rate-limiting step.

The Avrami model is a model used to evaluate the multi-step nature of the adsorption process. This model is defined by the following equation:

$$\ln[-\ln(1-\theta)] = \ln k_{AV} + n \ln t \quad (7)$$

Here $\theta = q_t/q_e$ represents the covering fraction, k_{AV} represents the rate constant and n represents the Avrami parameter. If $n<1$ and the resulting graph is linear, the process is considered to be diffusion

controlled. However, if the graph does not pass through the origin or the correlation coefficients are low, the validity of the model is considered limited.

The Weber–Morris model is an approach used to explain how gas diffuses through the internal pore structure of the adsorbent during the adsorption process. This model takes into account the movement of gas molecules within the porous structure of the adsorbent and the factors that affect the speed of this movement. The Weber–Morris equation is given as follows.

$$q_t = k_{dif} t^{1/2} + C \quad (8)$$

In this equation, k_{dif} represents the diffusion rate constant and C represents the boundary layer effect. If intraparticle diffusion is the only rate-determining step in the adsorption process, the relationship between q_t and $t^{1/2}$ is linear according to the Weber–Morris model and this line passes through the origin. If it does not pass through the correct origin, this indicates that the adsorption cannot be explained by intraparticle diffusion alone and that other mechanisms such as film diffusion or surface interactions also contribute to the process. If the adsorption mechanism consists of more than one step, more than one intersecting linear regions are observed in the q_t-$t^{1/2}$ plot. In this case, each linear region corresponds to different mechanisms.

The validity of the models was evaluated based on the regression coefficients (R^2); it was determined which kinetic model best represented the adsorption mechanism (Table 5). When compared according to the regression coefficients, Avrami and Boyd models showed low correlation coefficients for both biomass samples. While the R^2 values of the Boyd model varied between 0.2855-0.4988, these values remained between 0.5995-0.8443 for the Avrami model. These results show that the models in question cannot adequately represent the adsorption process.

Figure 7 shows the q_t – $t^{1/2}$ curves drawn according to the Weber–Morris model for horse chestnut shell and tangerine peel based activated carbon samples. The linear curves in the figure show that the data points fit the model line well, especially in the first region. This fit proves that surface adsorption is dominant in the first stage of the process. The fact that the linear curve does not pass through the origin at the beginning suggests that adsorption is not limited to intraparticle diffusion only; film diffusion or other surface-effect kinetics also contribute. In the second stage, the curve becomes more horizontal and the deviations increase. This indicates that adsorption becomes limited to intrapore diffusion in the later stages.

The R^2 values of the first stage of the Weber–Morris model are quite high (Table 5). In the horse chestnut peel sample, $R^2 = 0.9820$ at 80 bar pressure, and in the tangerine peel, $R^2 = 0.9775$ at the same pressure. These findings show that the first phase, namely the rapid surface diffusion step, is dominant in the adsorption process and that the adsorption rate is high in this phase. The low R^2 values of the second phase reveal that intraparticle diffusion occurs more slowly and in a dispersed manner. In this respect, the Weber–Morris model is a successful model in terms of representing the multi-stage structure of adsorption.

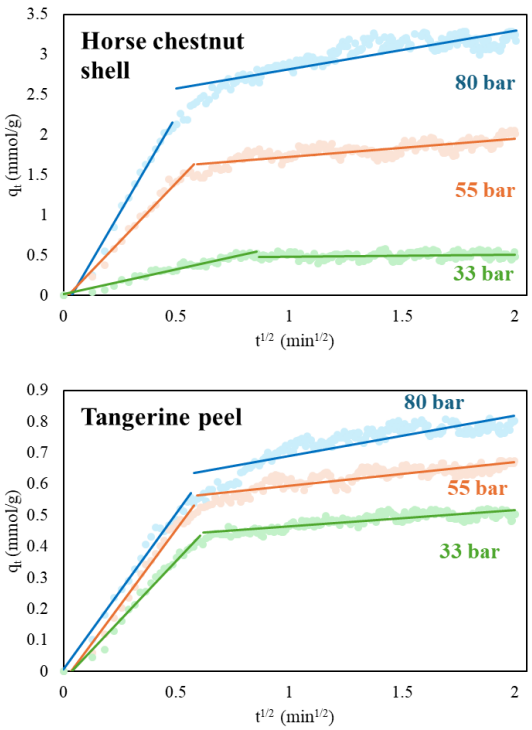

Figure 7. Weber-Morris curves for the adsorption of hydrogen on activated carbon surfaces

The kinetic parameters calculated according to the Weber–Morris equation also provide

important information about the nature of the process (Table 5). The k_1 value obtained at 80 bar pressure in the horse chestnut peel sample was 4.834 mmol g^{-1} $min^{-1/2}$, while this value was determined as 0.982 mmol g^{-1} $min^{-1/2}$ in the tangerine peel. This difference indicates that hydrogen molecules adsorb faster on the surface of the horse chestnut peel. In addition, a higher k1 value is associated with more active surface area and better mass transfer. A lower k_1 value in the tangerine peel may indicate that the pores are less accessible or have a more complex structure.

At the same time, the high rate constant observed in the first stage of the adsorption process suggests that hydrogen interacts quickly and easily with the active centers of the adsorbent. This situation can be directly related to the microporous structure of the surface. In the second stage, the very low k_2 values and the significant decrease in R^2 values indicate that this step is a kinetically slow process controlled by diffusion. As a result, it was determined that the model that best explains the adsorption kinetics of hydrogen on activated carbons is the Weber–Morris model. The high regression coefficients and curve fit of this model, especially for the first phase, indicate that the process is surface diffusion controlled and progresses in multiple steps. The kinetic parameters reveal that the adsorbent structure and pore distribution directly affect the adsorption rate. However, the Boyd and Avrami models are limited in understanding the adsorption process.

Table 5. Calculated kinetic parameters for the adsorption of hydrogen on the activated carbon surface

Sample name	P (bar)	Boyd			Pseudo-second order				Avrami		
		R^2	R	A	R^2_1	k_1	R^2_2	k_2	R^2	n_{AV}	K_{AV}
Horse chestnut shell	80	0.4536	1.28	-2.65	0.9820	4.834	0.7231	0.479	0.8093	0.4745	1.823
	55	0.4292	1.48	-2.84	0.9809	2.935	0.6255	0.222	0.7816	0.3452	1.664
	33	0.2855	1.12	-1.39	0.9432	0.613	0.0570	0.029	0.5995	0.3795	1.405
Tangerine peel	80	0.4988	1.18	-2.60	0.9775	0.982	0.7119	0.130	0.8443	0.5033	1.770
	55	0.4220	1.24	-2.55	0.9818	0.978	0.7269	0.076	0.8344	0.4413	1.911
	33	0.3948	1.18	-2.48	0.9824	0.765	0.7121	0.051	0.8409	0.5022	2.007

4. Conclusion

In this study, activated carbons derived from horse chestnut shell and tangerine peel were investigated for hydrogen storage. The horse chestnut-based carbon exhibited a superior capacity of 4.47 wt. % at 80 bar compared to tangerine peel (1.87 wt. % at 26 bar) due to its higher surface area and well-developed micropore structure, whereas the tangerine peel-based carbon showed lower performance. Among the isotherm models used in the evaluation of adsorption data, the Langmuir model showed the highest fit ($R^2 > 0.99$) for both biomass-derived adsorbents, thus revealing the tendency of hydrogen to adsorb as a single layer on homogeneous surfaces. Within the scope of kinetic analyses, it was determined that the pseudo-second-order and Weber–Morris models overlapped with the data to a high degree. As a result, biomass-derived activated carbons can be considered an effective and sustainable alternative in hydrogen storage applications with appropriate synthesis conditions.

This study demonstrates the hydrogen storage potential of biomass-derived activated carbons, marking a significant step in the evaluation of alternative materials that can contribute to sustainable energy systems. However, further development is needed to extend the results to a wider range of applications. A comparative study of carbons synthesized by varying the activation parameters of different biomass types (e.g., nut waste, agricultural pulp) is recommended. Furthermore, examining the adsorption behavior of not only hydrogen but also other gases such as methane and carbon dioxide is crucial for assessing the materials' potential for versatile applications. In addition, supporting physisorption data with electrochemical hydrogen storage tests will enable a combined interpretation of different storage strategies.

Article Information Form

The Declaration of Conflict of Interest/ Common Interest

No conflict of interest or common interest has been declared by the author.

Artificial Intelligence Statement

No artificial intelligence tools were used while writing this article.

References

[1] Z. Bicil, M. Doğan, "Characterization of activated carbons prepared from almond shells and their hydrogen storage properties," Energy & Fuels, vol. 35, no. 12, pp. 10227–10240, 2021.

[2] B. K. Kızılduman, "Kaolinit kilinin hidrojen depolama amaçlı kullanımı için modifikasyonu ve karakterizasyonu," BAUN Fen Bilimleri Enstitüsü Dergisi, vol. 25, no. 1, pp. 186–202, 2023.

[3] I. Dincer, C. Acar, "Review and evaluation of hydrogen production methods for better sustainability," International Journal of Hydrogen Energy, vol. 40, no. 34, pp. 11094–11111, 2015.

[4] E. E. Doğan, "Hydrogen production and its storage from solar energy," Advances in Materials Science, vol. 20, no. 2, pp. 14–25, 2020.

[5] M. Sevilla, A. B. Fuertes, "Sustainable porous carbons with a superior performance for CO_2 capture," Energy & Environmental Science, vol. 4, no. 5, pp. 1765–1771, 2011.

[6] G. W. Crabtree, M. S. Dresselhaus, and M. V. Buchanan, "The hydrogen economy," Physics Today, vol. 57, no. 12, pp. 39–44, 2004.

[7] E. E. Doğan, P. Tokcan, B. K. Kızılduman, "Storage of hydrogen in activated carbons and carbon nanotubes," Advances in Materials Science, vol. 18, no. 4, pp. 5–16, 2018.

[8] L. Schlapbach, A. Züttel, "Hydrogen-storage materials for mobile applications," Nature, vol. 414, no. 6861, pp. 353–358, 2001.

[9] A. Züttel, "Materials for hydrogen storage," Materials Today, vol. 6, no. 9, pp. 24–33, 2003.

[10] M. Doğan, A. Selek, O. Turhan, B. K. Kızılduman, Z. Bicil, "Different functional groups functionalized hexagonal boron nitride (h-BN) nanoparticles and multi-walled carbon nanotubes (MWCNT) for hydrogen storage," Fuel, vol. 303, 121335, 2021.

[11] Ü. Çakır, M. Doğan, B. K. Kızılduman, Z. Bicil, "Functionalized and Schiff base-based multi-walled carbon nanotubes for hydrogen storage," Journal of Alloys and Compounds, vol. 1010, 177290, 2025.

[12] M. Doğan, M. Y. Kalafat, B. K. Kızılduman, Z. Bicil, Y. Turhan, E. Yanmaz, et al., "Hydrogen storage analysis of fullerene and defective fullerenes: The first experimental study," Fuel, vol. 390, 134705, 2025.

[13] H. Barthélémy, M. Weber, F. Barbier, "Hydrogen storage: Recent improvements and industrial perspectives," International Journal of Hydrogen Energy, vol. 42, no. 11, pp. 7254–7262, 2017.

[14] Z. S. Doğan, E. E. Doğan, Z. Bicil, B. K. Kızılduman, "The effect of Li-doping and doping methods to hydrogen storage capacities of some carbonaceous materials," Fuel, vol. 396, 135280, 2025.

[15] M. Sevilla, N. Díez, A. B. Fuertes, "More sustainable chemical activation strategies for the production of porous carbons," ChemSusChem, vol. 14, no. 1, pp. 94–117, 2021.

[16] M. Doğan, P. Sabaz, Z. Bicil, B. K. Kızılduman, Y. Turhan, "Activated carbon synthesis from tangerine peel and its use in hydrogen storage," Journal of the Energy

Institute, vol. 93, no. 6, pp. 2176–2185, 2020.

[17] O. Ioannidou, A. Zabaniotou, "Agricultural residues as precursors for activated carbon production—A review," Renewable and Sustainable Energy Reviews, vol. 11, no. 9, pp. 1966–2005, 2007.

[18] A. Turkyılmaz, K. Isinkaralar, M. Doğan, B. K. Kızılduman, Z. Bicil, "Production, characterization, and hydrogen storage properties of activated carbon from horse chestnut shell," Sustainable Chemistry and Pharmacy, vol. 40, 101634, 2024.

[19] H. Jin, Y. S. Lee, I. Hong, "Hydrogen adsorption characteristics of activated carbon," Catalysis Today, vol. 120, no. 3–4, pp. 399–406, 2007.

[20] Z. Bicil, "Adsorption kinetics and mechanism of hydrogen on pristine and functionalized multi-walled carbon nanotubes," Fuel, vol. 403, 136130, 2026.

[21] S. Stelitano, G. Conte, A. Policicchio, A. Aloise, G. Desiderio, R. G. Agostino, "Pinecone-derived activated carbons as an effective medium for hydrogen storage," Energies, vol. 13, no. 9, 2237, 2020.

[22] H. Akasaka, T. Takahata, I. Toda, H. Ono, S. Ohshio, S. Himeno, H. Saitoh, "Hydrogen storage ability of porous carbon material fabricated from coffee bean wastes," International Journal of Hydrogen Energy, vol. 36, no. 1, pp. 580–585, 2011.

[23] N. Bader, O. Abdelmottaleb, "CO_2 activation of olive bagasse for hydrogen storage," Environmental Progress & Sustainable Energy, vol. 36, no. 1, pp. 315–324, 2017.

[24] S. H. M. Arshad, N. Ngadi, S. Wong, N. S. Amin, F. A. Razmi, N. B. Mohamed, A. A. Aziz, "Optimization of phenol adsorption onto biochar from oil palm empty fruit bunch (EFB)," Malaysian Journal of Fundamental and Applied Sciences, vol. 15, no. 1, pp. 1–5, 2019.

[25] M. Jung, J. Park, K. Lee, N. F. Attia, H. Oh, "Effective synthesis route of renewable nanoporous carbon adsorbent for high energy gas storage and CO_2/N_2 selectivity," Renewable Energy, vol. 161, pp. 30–42, 2020.

[26] R. C. Bansal, M. Goyal, Activated Carbon Adsorption. Boca Raton, FL, USA: CRC Press, 2005.

[27] C. T. Chiou, Partition and Adsorption of Organic Contaminants in Environmental Systems. Hoboken, NJ, USA: Wiley, 2003.

[28] A. O. Dada, A. P. Olalekan, A. M. Olatunya, O. J. Dada, "Langmuir, Freundlich, Temkin and Dubinin–Radushkevich isotherms studies of equilibrium sorption of Zn^{2+} unto phosphoric acid modified rice husk," IOSR Journal of Applied Chemistry, vol. 3, no. 1, pp. 38–45, 2012.

[29] P. Benard, R. Chahine, "Determination of the adsorption isotherms of hydrogen on activated carbons above the critical temperature of the adsorbate over wide temperature and pressure ranges," Langmuir, vol. 17, no. 6, pp. 1950–1955, 2001.

[30] J. Serafin, B. Dziejarski, C. Solis, P. R. de la Piscina, N. Homs, "Medium-pressure hydrogen storage on activated carbon derived from biomass conversion," Fuel, vol. 363, 130975, 2024.